Artificial Intelligence Approach to Damage Detection in Lightweight Structures

André Tavares
andregmtavares@tecnico.ulisboa.pt

Instituto Superior Técnico, Universidade de Lisboa, Portugal

July 2020

Abstract

Reliable and efficient damage detection is critical for the use of lightweight materials in the mechanical and aerospace industries. Within the context of Non-Destructive Testing (NDT), vibration-based tests have been applied for many decades to inspect components without damaging or debilitating their use. For posterior fault recognition, Artificial Intelligence techniques have achieved high success for a number of structural applications. In this work, Testing, Simulation and Artificial Intelligence have been combined in order to develop a defect detection procedure. The use of an Optomet Scanning Laser Doppler Vibrometer (SLDV) for such tests provides an interesting solution to measure the vibration velocities on the structure surface. The algorithms for identifying the defects are based on the Local Defect Resonance (LDR) concept, which looks to the high frequency vibrations to get a localized resonant activation of the defect. Artificial Intelligence (AI) techniques were implemented with the aim of creating an automatic procedure combined with feature extraction for damage detection. Wavelet transformation and modal analysis were used to provide inputs to the AI techniques. In order to better understand the limitation in terms of defect detection, damaged plates were modelled and simulated in order to perform a sensitivity analysis. Finally, an overall comparative overview of different algorithms results was also obtained.

Keywords: Lightweight plates, NDT, Laser Doppler Vibrometry, damage detection, AI

1. Introduction

Early detection of damages, whether in a production line or in a structural monitoring context can prevent significant economic expenses and major device malfunctions. The Local Defect Resonance (LDR) concept can be coupled with Non-Destructive Testing (NDT) techniques to get localized resonant activation of defects, by making use of high frequency excitations. This concept is based on the fact that a defect leads to a decrease in stiffness for a certain mass of the material in that area [1].

Machine Learning (ML) algorithms are feature classification techniques, that when applied to damage detection, can often achieve state-of-the-art results with automatic frameworks. In the Deep Learning (DL) subset of ML, a degree of feature learning is also offered by these techniques, where an algorithm learns a transformation or sequence of transformations of the raw data. Regarding signal analysis, deep neural networks have been used as classifiers for damage detection in beam structures [2], for fault recognition in the condition monitoring of rotating machinery and drivetrains [3][4], for psychoacoustic analysis [5] and other innovative non-engineering studies such as electrocardiogram classification [6]. Moreover, feature extraction techniques have been applied on time-signals to generate images that can be evaluated by DL algorithms for similar Structural Health Monitoring (SHM) applications [7]. Similar studies linking damage detection with image recognition have been done using deep neural networks for wind turbine fault classification ([8]) and autonomous crack detection ([9]).

In this work, within the context of NDT, with the contactless optical measurement technique Laser Doppler Vibrometer (LDV), ML and DL algorithms were developed for damage detection in lightweight plates. The proposed experimental analysis was done both in the frequency and time domains, where these algorithms were developed to analyse Frequency Response Functions (FRFs), time signals and also data obtained through feature engineering with modal analysis, Continuous Wavelet Transform (CWT) and Short-Time Fourier Transform (STFT). Furthermore, a simulation component was developed, where some ML algorithms were applied to data obtained through the simulation of damaged

plates.

2. Theoretical background

2.1. Local Defect Resonance (LDR)

Local Defect Resonance makes use of high frequency vibrations to get localized resonant activation of the defects. This concept is based on the fact that the inclusion of a defect leads to a decrease in stiffness for certain mass of the material in that area ([1], [10]). This phenomenon manifests itself in a particular natural frequency which can be defined as the LDR fundamental frequency.

Therefore, this technique implies an extension of traditional modal analysis frequency regimes to higher ones. The high frequencies associated with the localized defect activation provide high contrast between the defected and sound areas of the component [11]. The defects response measured at its resonance frequency highly surpasses the one obtained at the natural frequencies of the component. This strong wave interaction causes a strong rise of local temperature and non-linear behavior in the frequency band of the defect's response [12]. This concept has been used to improve defect localization and evaluation through ultrasonic thermography and shearography, along vibrometry methods.

2.2. Machine Learning

Machine Learning (ML) is a subset of Artificial Intelligence (AI) techniques that provides a computer program the ability to learn and improve from experience in reference to a specified task [13]. The practical use of a ML algorithm includes two phases. In a first phase, the algorithm is trained and in the second phase, the algorithm is used with prediction purposes. The training involves a set of data from which the algorithm is going to learn a certain task and the prediction involves a set of data to be analysed by the algorithm which will then output a prediction that ranges from the many purposes to which a ML algorithm can be applied. Two ML algorithms were used in this work, the K-means Clustering and the Multivariate Anomaly Detection, which will be described below.

2.2.1 K-means Clustering

The K-means Clustering is an unsupervised learning centroid based clustering algorithm. As unsupervised learning, this method works on an unlabelled training set, where each training example contains a certain amount of features but no labels. As a centroid based clustering algorithm it divides the training set into K different clusters. Therefore, the amount of clusters on which the data will be divided is an input to this algorithm.

Considering a dataset with m unlabelled training examples $\{x^{(1)}, x^{(2)}, ..., x^{(m)}\}$, where each example is a n sized vector of features ($x^{(i)} \in \mathbb{R}^n$), the aim of this algorithm is to aggregate the training examples into a pre-defined amount of clusters ($\mu_1, \mu_2, ..., \mu_K \in \mathbb{R}^n$). This process can be described in the following steps:

1. Random initialize K cluster centroids;
2. Repeat until all centroid positions remain constant {
   (a) Cluster assignment
   for $i = 1 : m$
   $c^{(i)} :=$ index(from 1 to K) of cluster centroid closest to $x^{(i)}$
   (b) Move centroid
   for $k = 1 : K$
   $\mu_{(k)} :=$ average of points assigned to cluster K
   }.

The process of randomly assigning K number of clusters which are randomly attributed to K training examples in the starting iteration of the algorithm implies some variability to this algorithm. It can happen that the clusters are luckily assigned near a global optima solution, or it can happen that the clusters are assigned to close points or near a local optima solution, which will freeze the iterative process of the algorithm. Therefore, this algorithm should be run for many random initialization and the best option should be identified as being the one which minimizes the cost function value J.

$$J(c^{(1)}, ..., c^{(m)}, \mu_1, ..., \mu_K) = \frac{1}{m} \sum_{i=1}^{m} \|x^{(i)} - \mu_{c^{(i)}}\|^2 \tag{1}$$

2.2.2 Multivariate Anomaly Detection

The Multivariate Anomaly Detection is a common type of ML used when the datasets contain an unbalanced number of examples between each class. It's used mainly for unsupervised learning problems, but contains some aspects of supervised learning. In situations where there is a considerable difference of training examples between classes, to train supervised learning algorithms like neural networks, would most likely end in having biased algorithms that make more classifications for the class with the largest amount of training examples. The Multivariate Anomaly Detection can overcome this problem, and is suitable to be applied in such situations.

This algorithm fits a Multivariate Gaussian distribution (equation 2) to the training set's features (x). After, through a threshold selection process,

the best threshold is obtained to separate training examples corresponding to anomalies from training examples representing common and acceptable values.

$$p(x, \mu, \Sigma) = \frac{1}{(2\pi)^{n/2}|\Sigma|^{1/2}} exp(-\frac{1}{2}(x-\mu)^T\Sigma^{-1}(x-\mu)) \quad (2)$$

Where;

$\mu = \frac{1}{m}\sum_{i=1}^{m} x^{(i)}$: mean vector of a feature's distribution ($\mu \in \mathbb{R}^n$).

$\Sigma = \frac{1}{m}\sum_{i=1}^{m}(x^{(i)} - \mu)(x^{(i)} - \mu)^T$: covariance matrix ($\Sigma \in \mathbb{R}^{n\times n}$).

The steps of the algorithm can thus be enumerated as:

1. Choose features, that might be indicative of anomalous examples;
2. Fit Multivariate Gaussian Distribution by calculating the mean vector μ and the covariance matrix Σ;
3. Given a new example x, compute $p(x)$;
4. Identify an anomaly if $p(x) < \epsilon$.

Where ϵ represents a constant threshold value from which an example may be assigned to an anomaly if its probability value is below this threshold. The selection of this threshold's value is usually calculated from a cross-validation subset of examples, by calculating which ϵ provides the most accurate anomaly predictions.

3. Experimental Analysis

In this section the experimental part of this work will be described. Several lightweight plate specimens of Carbon-Fiber Reinforced Polymer (CFRP) and PMMA with Flat Bottom Hole (FBH) defects were measured. In this section, emphasis will be given to the results for the PMMA plate. This lightweight plate contains eight FBH damages in the bottom surface and was measured looking at the top surface, where no traces of the defects can be visualized (Figure 1). Several algorithms will be presented in this work, which were developed with ML and DL techniques in order to analyse the measured data and detect the damages' location in the bottom surface of the plate. These algorithms are divided across a time-domain and frequency-domain analysis, which will be presented in the next sub-sections.

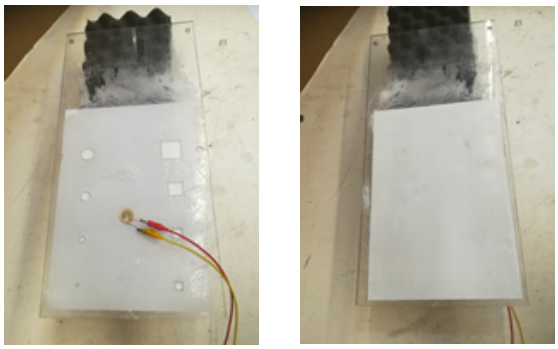

(a) Bottom plate surface with displayed damages.

(b) Top plate surface with no damages (the measured surface).

Figure 1: Measured PMMA plate with 8 damages.

3.1. Experimental Setup

The measurements were performed using an Optomet SWIR Scanning Laser Doppler Vibrometer (LDV). Figure 1 shows the measured PMMA plate, which was manufactured by bonding a polystyrene sheet of 300 x 210 x 0.5 mm^3 onto a 5 mm thick PMMA plate containing square and round holes of different sizes, using epoxy resin. It was excited with a piezoelectric patch up to a frequency of 40 kHz and measured with a grid of 2255 points (55x41) by the LDV. Moreover, an amplifier was used to enhance 50 times the generated signal by using a Falco Systems WMA-300. From these measurements, two types of data were obtained: Frequency Response Functions (FRFs) and time-signals, which are the starting steps for the frequency-domain and time-domain procedures described in this work.

3.2. Frequency-domain Procedures

The frequency-domain procedures are based on the acquired FRFs. As demonstrated in figure 2, two algorithms were developed: one Convolutional Neural Network (CNN) for the direct analysis of the FRFs; and one ML tool to analyse mode shape data or the consequent 2nd Derivatives. The algorithm behind the ML tool is developed by combining the K-means clustering and Multivariate Anomaly Detection, and it was named Gaussian Anomaly Detection Automated by Clustering (GADAC).

3.2.1 ML tool (GADAC)

This algorithm links the Local Defect Resonance (LDR) concept with an unsupervised learning clustering procedure in order to analyse data obtained from modal analysis performed using the Polymax tool in Simcenter Testlab® software [14].

This algorithm's methodology is presented in figure 3, along with the example of the absolute values

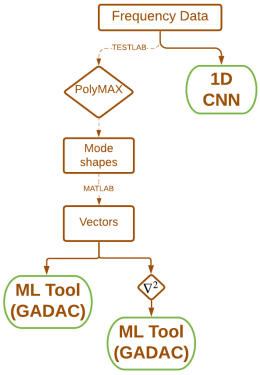

Figure 2: Frequency-domain algorithm procedure.

of a mode shape (each point relates to the vibration amplitude of one measured node on the plate). Whether from the mode shape or its 2nd Derivatives, a complex amplitude vector is the input to this algorithm. The first step, inspired on the LDR concept, is to cluster the highest amplitudes with K-means. A first defect map will be obtained from the output of this step, where the points whose amplitudes were assigned to the cluster with highest amplitudes will be classified as defected. This will serve as a reference for the Multivariate Gaussian Anomaly Detection to automatically select a threshold to classify the defected points based on their real and imaginary values. After this step, an improved defect map is obtained in comparison to the one after the first step.

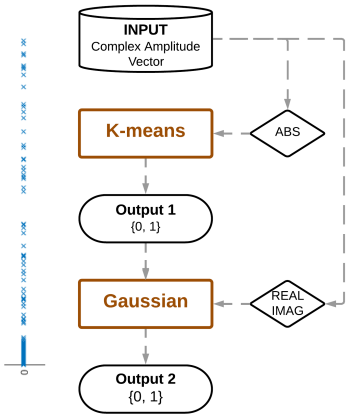

Figure 3: Frequency-domain ML tool (GADAC) method.

This procedure is repeated for all the mode shapes calculated in the 40 kHz frequency band experimentally measured with the LDV. This measurement was done with a grid of 2255 points (55x41), hence the mode shape motion is represented with an equivalent 55x41 grid of points. The final result of this algorithm will then be the sum of the algorithm's classification for each mode shape or its 2nd Derivatives. The aim of calculating the 2nd Derivatives of the mode shapes is to highlight the defect's presence in a mode shape (ϕ) making it easier to detect.

$$\frac{d^2\phi}{dx^2}; \frac{d^2\phi}{dy^2}; \frac{d^2\phi}{dxdy}$$

Figure 4 displays both the result for the application of this frequency-domain ML tool to the mode shapes (left) and to the 2nd Derivatives of the mode shapes (right). The plate measured in this study (figure 1) contains 8 damages, from which 6 were correctly detected in both these results, by observing the amount of positive defect classifications on the 3 bigger circular and squared plate defects. Moreover, some nodes were classified as damaged on the bottom left part of the defect maps. These are relevant to the location of where the piezoelectric patch was attached to the plate when making these measurements.

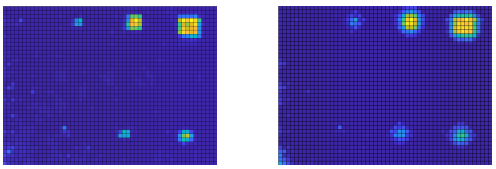

(a) mode shapes. **(b)** 2nd Derivatives.

Figure 4: Frequency-domain ML tool results.

3.2.2 1D CNN

A 1D Convolutional Neural Network (CNN) was developed to analyse the Frequency Response Functions (FRFs) containing the relation from the output vibration velocity and the input piezo patch's excitation force. The aim is to extract complex features from the FRFs with the CNN and classify whether they were measured on top of damaged or undamaged nodes. The LDV measures the plate's response to an excitation band of 40 kHz, therefore, in order to have a meaningful number of spectral lines for the FRF calculation, these end up being a vector containing a significant amount of points (around 7k for these measurements). It is impractical to design a 1D CNN to properly perform feature extraction and recognition from the analysis of the entire FRF taken as a single input. Thus, a pre-processing step was implemented to segment the signal into smaller equally sized segments. Moreover, this segmentation operation was performed with a certain overlap of one segment to another. This resulted in a data augmentation technique which enhances the amount of data to train the algorithm, which is crucial for DL applications.

Figure 5 illustrates the steps of implementing the developed algorithm, where the pre-processing contains precisely the two operations described above: segmentation and overlap. Moreover, it shows an example of a measured FRF.

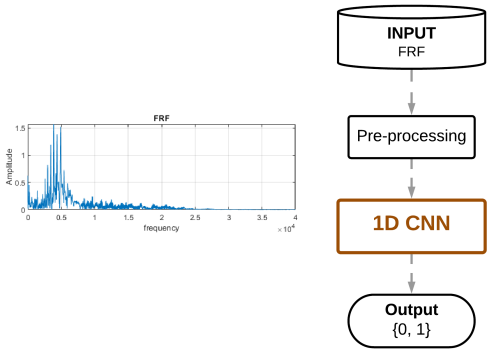

Figure 5: Frequency-domain 1D CNN method.

The architecture of the 1D CNN was designed with a manual procedure to optimize the number of layers and their parameters. The kernel sizes and number of convolutional pooling blocks was studied taking into reference the accuracy of the obtained results. The chosen architecture is made of 5 convolutional, batch normalization, ReLU, pooling layer blocks, followed by one fully connected (200 neurons) and dropout layer, ending with a softmax layer. The convolutional layers' kernel sizes were defined with 3 neurons, except for the first which had 61. This choice of a wide first-kernel was made to better suppress the high frequency noise.

Contrary to the previously presented ML tool, which is an unsupervised learning algorithm, the 1D CNN is supervised learning. Hence, to train this algorithm there is the need for labels, which is a hard task, since it is very difficult to have the ground-truth on which LDV measured nodes are on top of defects or otherwise. The plate is measured on the top surface, which is a clean undamaged surface, with no regards whatsoever for where the 2255 measured node grid is, in relation to the damages on the bottom surface. Therefore, for this and the other supervised learning algorithms used in this work (the CNNs), fifty percent of the classification labels obtained from the results with the time-domain ML tool (sub-section 3.3.1) were considered to train the algorithm (figure 9 a)). Hence, a ML algorithm is used to train another and enable continuing the proposed investigation, for this case in which obtaining the ground-truth labels is so far deemed impractical.

The classification results on the LDV measurement done with a 2255 node grid (55x41) is shown in figure 6, where the classification of nine groups of yellow points is achieved. These points are the ones

Figure 6: Frequency-domain 1D CNN results.

detected as damaged, whereas all points in blue are detected as non-damaged. Considering the PMMA plate has 8 defects, the image shows the defect map obtained with this algorithm where an accurate classification of 7 out of 8 damages is achieved. The group of points in the bottom left corner of the map corresponds to the detection of the piezoelectric patch's location, where the excitation was provided to the plate. However, there is a ninth defect detected in the middle of the plate to the left, which corresponds to a misclassification. All in all, the smaller circular defect wasn't detected.

3.3. Time-domain Procedures

The time-domain procedures originate from the analysis of the time-signals measured with the LDV, which record the vibration velocity for each measured point during the excitation period. As shown in figure 7, three algorithms were developed: two with Convolutional Neural Networks (CNNs), with 1D and 2D inputs (time-signal vectors and CWT or STFT images, respectively); and one with the ML K-means clustering tool. A pre-processing step was done in MATLAB with the Continuous Wavelet Transform (CWT) and with the Short-Time Fourier Transform (STFT). These two time-frequency transformations provide an analysis of the time-varying spectral characteristics, useful for detecting defected node's measurements. Since the vibration of a defected node will be different than that of a non-defected node, both CWT and STFT can capture this phenomenon, thus being optimal feature extraction techniques for ML applications. They were used to extract time-frequency image representations (input to the 2D CNN), and also to calculate the maximum vibration amplitude per measured point by the LDV (input to the ML tool K-means). In this subsection, these algorithm methodologies will be briefly explained and their results presented.

3.3.1 ML tool (K-means)

By applying the CWT or the STFT to the signals, the maximum amplitude of vibration for each measured point can be obtained. Hence, the output from both transformations (as shown in figure 7) is a vector of amplitudes, with as many points as there were measured nodes (2255 as referenced in

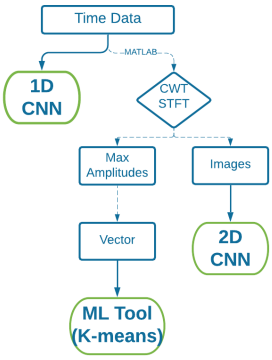

Figure 7: Time-domain algorithm procedure.

sub-section 3.1). According to the LDR concept, the highest amplitudes will be relevant to the damaged points on the plate. This algorithm clusters the amplitudes from the vector in two clusters of points. The one with the highest amplitudes will be classified as containing the damaged nodes of the plate. This methodology is illustrated in figure 8, along with an example representation of the obtained vector of points from either the CWT or STFT. Additionally to the K-means clustering step, there was implemented a filter to remove the defects detected with one single node, which correspond to outliers likely resultant from measured points with low signal-to-noise ratio, by the LDV. Thus, this algorithm has a resolution of two nodes per defect.

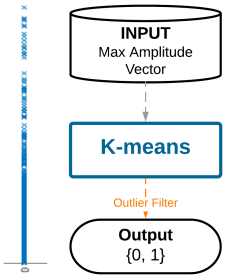

Figure 8: Time-domain ML tool (K-means) method.

Figure 9 displays this algorithm's results for both the CWT and STFT input max amplitude vectors. Both defect maps have a binary classification where the nodes in yellow correspond to the defected nodes and the blue to the non-defected. The PMMA measured plate (figure 1) contains 8 defects, hence the optimal result would be detecting eight groups of yellow points in the regions where the defect are located in the plate. Both these algorithm's classifications, represented in figure 9, allow to detect 5 damages, the three biggest squared and two biggest circular ones.

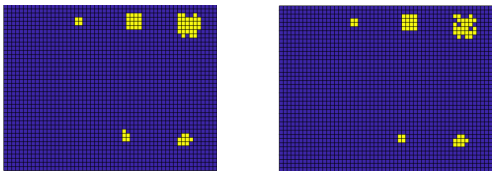

(a) CWT. **(b)** STFT.

Figure 9: Time-domain ML tool results.

3.3.2 2D CNN

Alternatively to calculating the maximum vibration amplitudes, the application of both transformations was used to generate time-frequency image representations of each transformation applied to each time-signal. The transformations were saved as Red Green Blue (RGB) images, one per each time-signal, hence one per each measured node. Figure 10 shows two examples of these images: to the left, the frequency-time representation of the Continuous Wavelet Transform (CWT); to the right, the time-frequency representation of the Short-Time Fourier Transform (STFT). In both images, a line in brighter color, which corresponds to the sine-sweep used as excitation to the PMMA plate up to 40 kHz can be highlighted. This algorithm analyses each of these images with a 2D CNN and classifies whether the signal is measured on top of damaged nodes or otherwise (binary classification). Moreover, the same outlier filter methodology applied in the algorithm previously described (sub-section 3.3.1) was applied to this algorithm. In this way, defects detected with just one node are attributed to outliers and discarded (this algorithm also has a two damaged nodes per defect resolution).

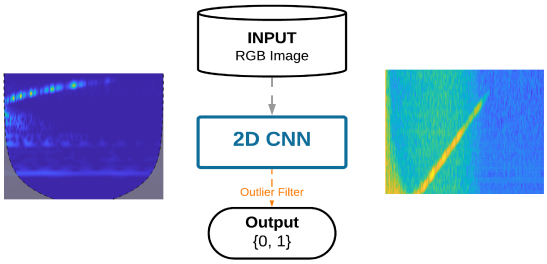

Figure 10: Time-domain 2D CNN method.

A previously developed CNN architecture was used and trained to this damage detection purpose the GoogLeNet [15]. In order to train it, fifty percent of the labels from the 5 defects map result (figure 9 a)) obtained with the ML tool for the CWT max amplitudes (sub-section 3.3.1) were used. The results from the 2D CNN are presented in figure 11.

This algorithm detected 6 out of the 8 defects in

the PMMA plate (figure 1), plus the piezo patch's location (bottom left corner), for both the CWT and STFT images. Only the two smaller circular defects were left undetected. Whereas the 2D CNN's classification for the STFT images only classifies the existing damages and the excitation's location, the classification for the CWT images provided some misclassifications. Above the piezo patch's location, there were detected some damaged nodes where in fact there are none, and the same for a misclassification on top of the smaller circular defect detected. Hence, it can be concluded that the STFT images provide a more reliable dataset to be classified with a 2D CNN for the damage detection purpose.

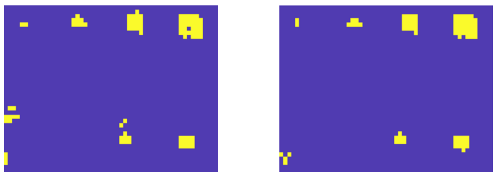

(a) CWT. **(b)** STFT.

Figure 11: Time-domain 2D CNN results.

3.3.3 1D CNN

Similarly to the developed methodology for the frequency domain procedure, explained previously in the sub-section 3.2.2, a 1D Convolutional Neural Network (CNN) was developed to analyse the one-dimensional time-signal vectors containing the vibration time history of each measured node. The LDV measures these signals with a high-frequency sampling rate (to cope with the high-frequency dynamic behaviour), hence the signals obtained contain almost 12k samples. Therefore, the same pre-processing step described in sub-section 3.2.2 was applied to this algorithm, in order to truncate the time-signal vectors into equally sized segments, with a certain overlap. The overlap operation, with which the segmenting is performed, is a data augmentation procedure, which contributes to the training of this algorithm. Figure 12 shows this algorithm's methodology and an example of a measured time-signal. The aim will be to classify whether these were measured on top of a damaged node or otherwise.

In terms of architecture, the same used for the analysis of the FRFs was used in this case (described in sub-section 3.2.2) and to train it, equally fifty percent of the labels obtained from the ML tool results on the CWT max amplitudes (figure 9 a)). Its classification result on the same measurement as all the previously presented algorithms is shown in figure 13, where the accurate classification of 7 out

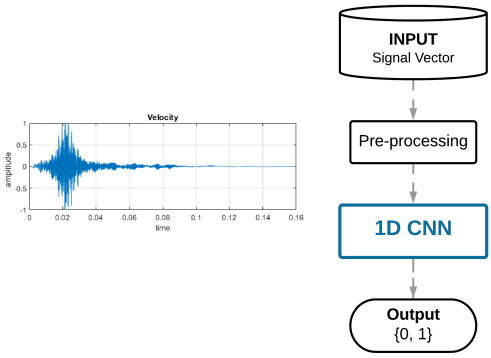

Figure 12: Time-domain 1D CNN method.

of the 8 damages in the PMMA plate is achieved, plus the location of the piezoelectric patch. The smallest circular defect was left undetected equally to the results from the previous algorithms.

Figure 13: Time-domain 1D CNN results.

3.4. Match of all techniques

In the experimental analysis section, several algorithms were presented for both frequency-domain and time-domain data. The results for each algorithm were presented on a single dataset obtained from one measurement of the PMMA plate with the LDV. A comparison of the algorithm's performance and accuracy of detection on the same dataset are presented in table 1 and will be commented in this sub-section.

Table 1 shows that either considering the CWT and STFT data for the ML tool and 2D CNN algorithms, the accurate number of defects detected is the same (5 defects for the ML tool and 6 defects for the 2D CNN). However, as previously commented in sub-section 3.3.2, the classification for the CWT images with the 2D CNN provided some misclassifications which didn't occur for the STFT image classification. Comparing the results from the time-domain ML tools to the frequency-domain ML tools, the detection of one more defect (the second smallest circular defect) was obtained.

Passing from ML to the DL algorithms, an enhancement of defects detected can be highlighted. The algorithms which provided the best classification results were the 1D CNNs, which detected 7 defects (plus the location of the piezoelectric patch's excitation) both for the analysis of the time-signals and Frequency Response Functions (FRFs).

However, for the frequency-domain 1D CNN, one misclassification was outputted by the algorithm, which didn't happen for the time-domain. All in all, only the smallest (circular) defect was left undetected, in the PMMA plate with 8 defects.

Table 1: Sum-up of the algorithms' results

Time-Domain		Frequency-Domain	
Method	Results	Method	Results
ML tool - CWT	5 defects	ML tool	6 defects
ML tool - STFT	5 defects		
2D CNN - CWT	6 defects	ML tool - 2nd Grad	6 defects
2D CNN - STFT	6 defects		
1D CNN	7 defects	1D CNN	7 defects

4. Simulation Analysis

Secondly to developing an experimental analysis, a simulation analysis was created in order to study the potentialities of certain algorithms to data obtained through Finite Element Analysis (FEA). Similarly to the modal analysis experimental procedure in figure 2, the mode shapes of the modelled damaged plate were calculated (Figure 14). A similar ML tool methodology to the one presented for the analysis of the experimental mode shapes and their 2nd Derivatives was developed using the K-means algorithm. The reason behind not applying the ML tool (GADAC), similarly to the experimental analysis, lies in the fact that mode shapes calculated through FEA are represented by real and not complex numbers.

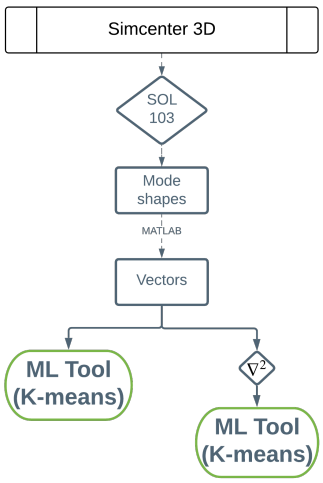

Figure 14: Simulation analysis algorithm methodology.

4.1. Simulation Setup

The FEA was performed using Siemens Simcenter 3D® software, to obtain the mode shape displacement for several modes in a frequency interval between 0 and 40 kHz. The choice of such a high frequency band goes in agreement with the LDR concept, in order to obtain the vibration behaviour for high frequency modes, which are dominated by the defected region vibration. Considering the Finite Element (FE) model, a squared plate was created (120x120 mm) with two squared defects (side of 20 and 10 mm) and two circular defects (diameter of 20 and 10 mm), as shown in Figure 15. The defects themselves were simulated as Flat Bottom Holes (FBHs), by accordingly reducing the thickness of the plate in the defects' areas. In order to obtain the mode shapes, the SOL 103 - Real Eigenvalues was used with free-free boundary conditions. An example of a LDR mode can be seen in Figure 15, and distinguished by the high localized vibration amplitude in one of the defect's locations. Within the 40 kHz frequency band from which the mode shapes were calculated, more than 400 mode shapes were obtained with a fine mesh.

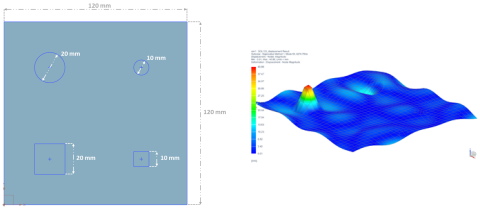

Figure 15: Modelled plate and a Local Defect Resonance mode obtained with FEA

4.2. ML tool

The working principles of this algorithm are linked to the LDR concept, since K-means is implemented to cluster the highest vibration amplitudes from the mode shapes in order to relate them to the damaged points. Each mode shape is characterized by a vector of points (represented in figure 16), where each point is equivalent to the vibration displacement in a specific node of the plate. The highest amplitudes will be related to the damage's vibration, hence relating the points clustered with the highest amplitudes to being defected will provide the insights for the localization of the damages in the plate. The methodology described here is shown in figure 16, where K-means runs with three clusters. Thus aiming to have one cluster for the points with close to zero amplitude, one for the low amplitudes related to lower vibration in healthy parts of the plate and a last cluster to obtain the points with the highest amplitude which will be related to the damage vibration.

For one of the methodologies, a 2nd Derivatives

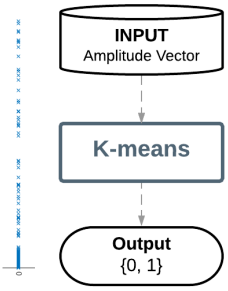

Figure 16: Machine Learning tool method.

step was implemented previously to the clustering procedure, aiming to enhance the influence of the defect in a mode shape, making it easier to detect (figure 14). The results of this application can be seen in Figure 17, where a mode shape is compared with its corresponding result after the 2nd Derivative. It can be seen that, from a high frequency mode shape of combined plate and defect vibration, the results after the 2nd Derivatives highlight the four defects, making them more easily detectable.

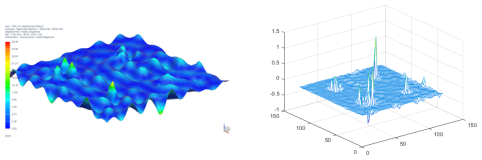

Figure 17: Influence of the 2nd Derivatives on a mode shape

Figure 18 shows the results obtained with the ML tool (K-means), on both the mode shapes and its 2nd Derivatives obtained for a plate with 30% of thickness in the defected areas. This algorithm runs independently for each mode shape or consequent 2nd Derivatives, and the final result is a sum of all single outputs. Not only were the four defects detected, but also important considerations regarding their shape managed to be retrieved.

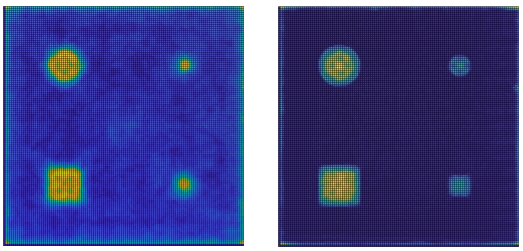

(a) Mode shapes. **(b)** 2nd Derivatives.

Figure 18: Machine Learning tools' results.

5. Conclusions

In this work, Machine Learning and Deep Learning techniques were implemented to perform damage detection in lightweight plates. Some of these techniques were combined with feature extraction engineering with modal analysis and time-frequency transformations. Furthermore, the physical concept of Local Defect Resonance was combined with the algorithms to build an enhanced damage detection methodology. In the experimental analysis, a broad study of different time and frequency domain procedures was developed, from which the success of implementing ML and DL techniques for damage detection can be concluded. Comparing all techniques, the 1D CNNs provided the best damage detection results. All in all, the developed algorithms managed to detect almost all damages. The simulation analysis further presented in this work allowed to study the performance of the ML tool (K-means) on data obtained with Finite Element Analysis. The algorithm not only managed to detect the damages, but also captures important considerations of their shapes.

References

[1] I. Solodov, M. Rahammer, and N. Gulnizkij, "Highly-sensitive and frequency-selective imaging of defects via local defect resonance," in *Proceedings of European Conference on Non-destructive Testing (ECNDT 2014)*, vol. 6, 2014.

[2] O. Abdeljaber, O. Avci, S. Kiranyaz, M. Gabbouj, and D. J. Inman, "Real-time vibration-based structural damage detection using one-dimensional convolutional neural networks," *Journal of Sound and Vibration*, vol. 388, pp. 154–170, 2017.

[3] Z. Chen, K. Gryllias, and W. Li, "Intelligent fault diagnosis for rotary machinery using transferable convolutional neural network," *IEEE Transactions on Industrial Informatics*, vol. 16, no. 1, pp. 339–349, 2019.

[4] F. Jia, Y. Lei, J. Lin, X. Zhou, and N. Lu, "Deep neural networks: A promising tool for fault characteristic mining and intelligent diagnosis of rotating machinery with massive data," *Mechanical Systems and Signal Processing*, vol. 72, pp. 303–315, 2016.

[5] B. Lopes, C. Colangeli, K. Janssens, A. Mroz, and H. Van der Auweraer, "Neural network models for the subjective and objective assessment of a propeller aircraft interior sound quality," in *INTER-NOISE and NOISE-CON Congress and Conference Proceedings*, vol. 259,

pp. 4124–4135, Institute of Noise Control Engineering, 2019.

[6] S. Kiranyaz, T. Ince, and M. Gabbouj, "Real-time patient-specific ecg classification by 1-d convolutional neural networks," *IEEE Transactions on Biomedical Engineering*, vol. 63, no. 3, pp. 664–675, 2015.

[7] J. C. Aldrin and D. S. Forsyth, "Demonstration of using signal feature extraction and deep learning neural networks with ultrasonic data for detecting challenging discontinuities in composite panels," in *AIP Conference Proceedings*, vol. 2102, p. 020012, AIP Publishing LLC, 2019.

[8] A. Shihavuddin, X. Chen, V. Fedorov, A. Nymark Christensen, N. Andre Brogaard Riis, K. Branner, A. Bjorholm Dahl, and R. Reinhold Paulsen, "Wind turbine surface damage detection by deep learning aided drone inspection analysis," *Energies*, vol. 12, no. 4, p. 676, 2019.

[9] C. V. Dung *et al.*, "Autonomous concrete crack detection using deep fully convolutional neural network," *Automation in Construction*, vol. 99, pp. 52–58, 2019.

[10] I. Solodov, "Resonant ultrasonic imaging of defects for advanced non–linear and thermosonic applications," *International Journal of Microstructure and Materials Properties*, vol. 9, no. 3-5, pp. 261–273, 2014.

[11] J. Segers, S. Hedayatrasa, E. Verboven, G. Poelman, W. Van Paepegem, and M. Kersemans, "Efficient automated extraction of local defect resonance parameters in fiber reinforced polymers using data compression and iterative amplitude thresholding," *Journal of Sound and Vibration*, vol. 463, p. 114958, 2019.

[12] I. Solodov, J. Bai, S. Bekgulyan, and G. Busse, "A local defect resonance to enhance acoustic wave-defect interaction in ultrasonic nondestructive evaluation," *Applied Physics Letters*, vol. 99, no. 21, p. 211911, 2011.

[13] T. M. Mitchell *et al.*, "Machine learning," 1997.

[14] B. Peeters, H. Van der Auweraer, P. Guillaume, and J. Leuridan, "The polymax frequency-domain method: a new standard for modal parameter estimation?," *Shock and Vibration*, vol. 11, no. 3, 4, pp. 395–409, 2004.

[15] C. Szegedy, W. Liu, Y. Jia, P. Sermanet, S. Reed, D. Anguelov, D. Erhan, V. Vanhoucke, and A. Rabinovich, "Going deeper with convolutions," in *Proceedings of the IEEE conference on computer vision and pattern recognition*, pp. 1–9, 2015.